CWE-8
June 7-11, 2026
London, ON, Canada

Evaluation of Heat Stress and Hot Environment in the Tokyo Metropolitan Area on an Extreme Hot Day in 2018

Maiko Arai [a], Tetsuro Tamura [b], Hidenori Kawai [c]

[a]*Taisei Corporation, 344-1, Nase-cho, Totsuka-ku, Yokohama, Japan, arimik00@pub.taisei.co.jp*
[b]*Yokohama National University, 79-7, Tokiwa-dai, Hodogaya-ku, Yokohama, Japan, tamura-tetsuro-dr@ynu.ac.jp*
[c]*Ochanomizu University, 2-1-1 Otsuka, Bunkyo-ku, Tokyo, Japan, kawai.hidenori@ocha.ac.jp*

SUMMARY

Recently, it is important to evaluate heat risk for the prevention of heatstroke in urban areas. In this study, we use the method for LES coupling with radiation and conduction model in Tokyo on an actual extremely hot day in summer. The inflow turbulence was considered meteorological disturbances and atmospheric stability based on the WRF-LES result.

The analysis results were compared with the observation data at Kitanomaru in Tokyo, Japan, the weather observatory, and confirm the accuracy of the prediction. WBGT was more than 31°C ("danger" rating) occurred intermittently in low-velocity areas, for examples, in the sunny and wake area of high-rise building.

Keywords: *Extreme hot day, Meteorological disturbance, WRF-LES, LES, Thermal radiation analysis*

1. INTRODUCTION

In recent years, extreme hot days has become a significant problem in summer, making the evaluation of heat stress related to heatstroke risks increasingly important. On July 23, 2018, record-breaking heat was observed primarily in the Kanto and Tokai regions in Japan, with temperatures exceeding 40°C even in Tokyo.

For the evaluation of heat stress, Computational fluid dynamics (CFD)-based simulation techniques are being utilized to predict the thermal environment in urban districts. It is important to improve the accuracy of conventional time-averaged prediction, as to predict unsteady, non-isothermal phenomena such as the interaction between turbulent and radiative fields at the urban scale and the frequency of localized high-temperature events. From the perspective of risk assessment, for example, in dispersion analysis of air pollutants, it is necessary to consider peak pollutant concentrations when evaluating their impacts on human health. Therefore, large-eddy simulation (LES) has been employed to capture transient high-concentration events (Nozu and Tamura, 2012). Similarly, in heatstroke risk assessment, it is considered important to consider not only average values but also transient characteristics, such as the occurrence and frequency of localized high temperatures, the accumulation of heat stress in the human body, and the duration of exposure.

Previous studies (for example, Y. Cui et al., 2020) that have focused on the relationship between heatstroke caused by high temperatures and emergency transports due to heart disease caused by extreme temperatures have suggested that analyses based solely on daily temperature data are insufficient. Instead, hourly-scale analyses and evaluations of the cumulative heat stress over periods ranging from several hours to several days are required. However, since LES analysis

covering several days is difficult with current computational capabilities, the present study aims, as an initial step, to predict transient thermal environments over short time periods.

Indicators for heat risk assessment include international standards such as ISO 7933 (2018) and the UTCI (Universal Thermal Climate Index), which incorporates human physiological responses. Among these, the Wet-Bulb Globe Temperature (WBGT) is a commonly used index. WBGT is a weighted average based on outdoor measurements and can be easily obtained. WBGT is considered to have a higher correlation with the number of heatstroke-related emergency transports than air temperature and is also utilized on the Ministry of the Environment of Japan's heatstroke prevention information website (2025 accessed).

Focusing on high-temperature occurrences in the Tokyo metropolitan area, the authors considered that regional meteorological scale's velocity and temperature fluctuations significantly impact the thermal environment within the urban canopy. To predict detailed non-isothermal phenomena at the urban scale, first, we conducted regional meteorological simulations using the regional meteorological model Weather Research & Forecasting Model (WRF) and WRF-LES, reproducing the meteorological field during the intense hot day of July 2018 in Tokyo. Next, we generated inflow turbulence considering meteorological disturbances during the same hot day using a method from Arai et al., (2025). And we used these to conduct coupled analysis of the turbulent flow and radiation field in the Tokyo metropolitan area. Furthermore, as an evaluation of heat stress in densely built-up urban areas, we attempted to evaluation the unsteady characteristics of WBGT for preventing heatstroke.

2. ANALYSYS METHOD

2.1. The method for LES coupling with radiation and conduction model in an actual urban area

In this study, first, the meteorological fields for the target day were reproduced using the regional meteorological models WRF and WRF-LES. Next, inflow boundary conditions for the simulation in the urban district were generated using two approaches: the spatial filtering and rescaling method by Kawai and Tamura (2020) and the method by Arai et al. (2025), which generates inflow turbulence considering meteorological disturbances during an actual extreme hot day by employing two driver regions performing non-isothermal Large Eddy Simulation (LES).

In this study, coupled analysis of turbulent flow and radiation fields (Arai et al., 2024a) was performed as a method to reproduce the heat dissipation process from complex urban surfaces (Figure 1,2). FrontFlow/Red was used as the solver for the finite volume method (FVM) based on unstructured grids. In the thermal radiation analysis, long-wavelength radiation was calculated by solving the transport equation for radiative intensity using the finite volume method. To account for the interaction between heat transfer and the turbulent flow field in the coupled analysis of the turbulent flow field and thermal radiation/conduction, the heat conduction calculation was performed at the same time step as the LES.

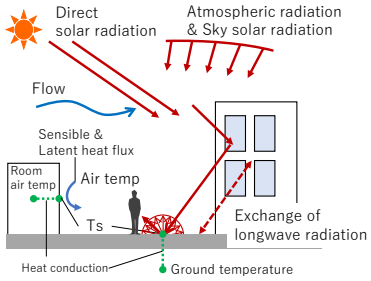

Figure 1: Calculation of the thermal radiation using radiation transport equation

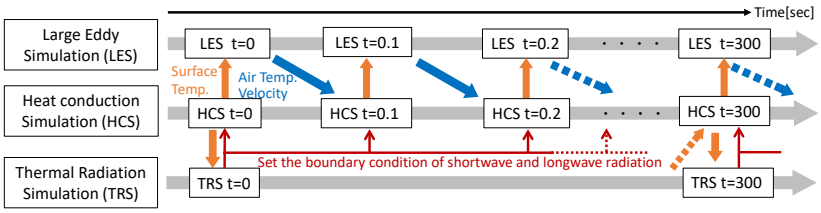

Figure 2: Coupling process of LES, heat conduction, and thermal radiation analysis

2.2. The method for generating inflow turbulence considering temperature instability based on the urban meteorological disturbances

The extremely hot day in Tokyo on July 23, 2018, target in this report, is possible to be influenced by the convection of hot air from the meso-meteorological scale. WRF-LES results show a grid-like structure in the horizontal cross-section of the temperature distribution. In such conditions, where thermal effects are particularly strong and the atmosphere near the ground is locally unstable, the influence of velocity and temperature fluctuations originating from the meteorological field is also considered significant. Thus, rather than assuming conventional fluid dynamic boundary layer profiles, it is necessary to generate inflow turbulence that account for meteorological disturbances based on the results of meso-meteorological model. In this study, we applied a method for generating inflow turbulence that account for urban meteorological disturbances (Arai et al., 2025) for predicting unstable thermal fields such as those on extremely hot days.

The generation process is three steps: **(1)** Generation of spatial-temporal data of the atmospheric boundary layer using WRF-LES, **(2)** addition of high-frequency fluctuation components using a spatial filtering and rescaling method (Kawai and Tamura, 2020) (Region 1), and **(3)** a non-isothermal LES analysis (Region 2) in which the vertical temperature distribution for the target time period from WRF-LES is applied to the inflow surface. Here, calculations are performed assuming that the boundary layer height corresponds to the part of the WRF-LES potential temperature distribution where it remains constant (neutral condition). The inlet condition of temperature in Region2 was set by dimensionless conversion as in Eq. (1), based on the temperature difference between the temperature at the boundary layer thickness (θ_m , the temperature that became uniform within the boundary layer), and the temperature at the bottom surface (θ_{bot}).

$$\theta^* = \frac{\theta - \theta_m}{\theta_{bot} - \theta_m} \tag{1}$$

The temperature boundary condition at the bottom surface was assumed to be unstable, reflecting ground warming by solar radiation during summer daytime. So, we set $\theta^* = 1$, a Dirichlet condition. Furthermore, the Richardson number (Eq. (2)), one of the indexes of atmospheric stability, was used as a parameter for the buoyancy term. Here, g is the gravitational acceleration, $\beta(= 1/\theta_0)$ is the volume expansion coefficient, θ_0 is the reference temperature, $\Delta\Theta$ is the difference of representative temperature , δ is the boundary layer height, In this case, $U = u_\tau$was taken as the representative velocity (friction velocity).

$$Ri = g\beta\frac{\Delta\Theta\delta}{U^2} \tag{2}$$

The procedure for generating inflow variation winds is shown in Figure 3. This method enables the generation of inflow turbulence considering thermal condition based on and the results of the mesoscale meteorological model.

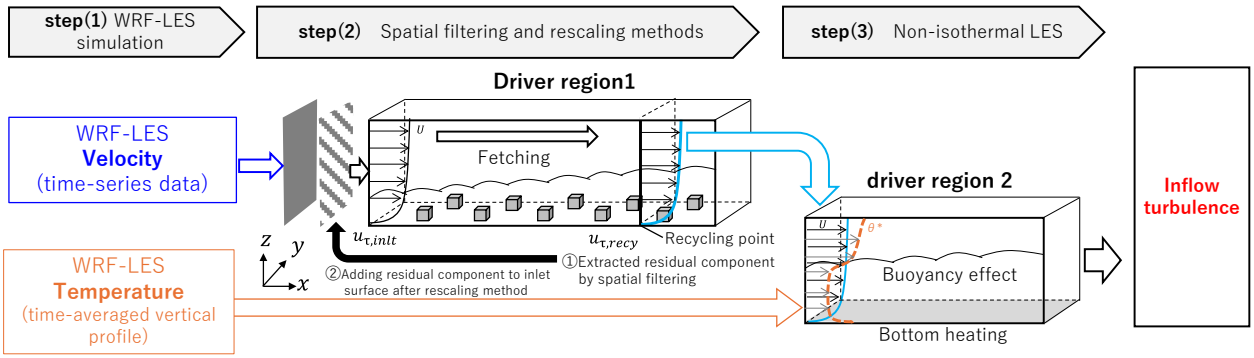

Figure 3: Conceptual diagram of the method for generating inflow turbulance

3. SIMULATION OF THERMAL ENVIRONMENT IN AN EXTREME HOT DAY

3.1. Overview of Analysis condition and simulation results

A coupled analysis of the turbulence flow and radiation field was conducted for the period from 11:32 to around 12:00 on July 23, 2018, when the Kanto area experienced record-breaking hot. The prevailing wind direction during the target period was north-northwest. The analysis domain included the Tokyo District Meteorological Observatory (at Kitanomaru Park). The analysis domain is shown in Figure 4. Boundary conditions for buildings and ground surfaces were classified into buildings, roads, grass surfaces, concrete surfaces, etc., with thermal properties assigned to each. The analysis conditions and the boundary conditions are shown in Table 1,2.

Figure 5 shows the analysis results. The colors of the buildings and ground surface represent surface temperature distributions, and the vertical cross-section shows the air temperature distribution. The wind flowing onto the sidewalk along the main road, which extends in an east-west direction, is indicated by white streamlines. From the surface temperature data, differences in surface temperature due to variations in the materials of the road, other ground surfaces, and buildings can be observed. On the main road in the sunny part of the urban area, the surface temperature was approximately 60–65°C. Additionally, the wind flowing in from the left side of the figure seems to form small vortex structures along the main road. In the next section, we will attempt to evaluate the thermal environment within this urban district, where such complex flow patterns are formed.

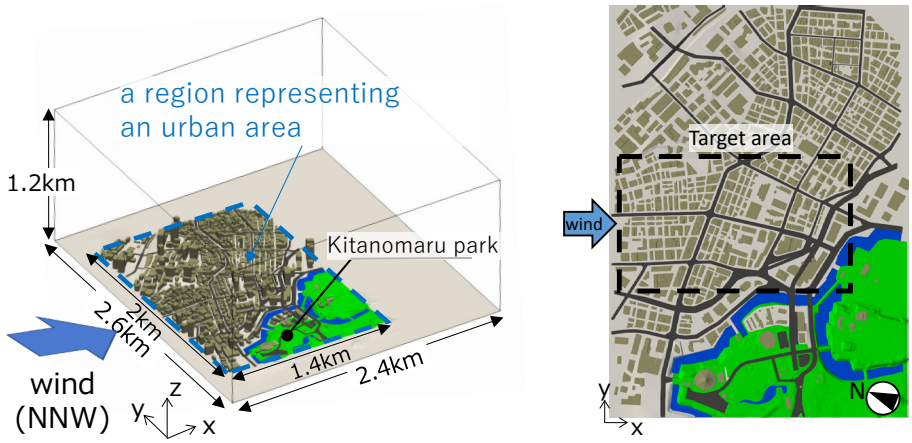

(a) Analysis area (b) Expansion figure of urban area

Figure 4: Analysis model

Table 1 Analysis conditions

Target period	About 28 minutes (July 23, 2018, 11:32 ~ 12:00) **With preliminary simulation for about 24.5hr* *(Only thermal conduction and radiation)*
Weather condition, wind direction	Sunny day, NNW
Time interval (dt)	LES, thermal conduction: 0.1 sec, longwave radiation, solar radiation (sun's movement): 5 minutes
Analysis grid	Total number of grid cells: about 60 million, Tetra mesh (node-centered) Minimum grid size: 1 m on the surface, 0.2 m × 3 layers in the boundary layer
Analysis area size	2.4km (streamwise)×2.6km (spanwise)×1.2km (vertical) (Reproduction area of buildings: 1.4km (stream)×2km (span))
Algorithm	SMAC method
Time integration	Euler implicit
Spatial discretization	2nd order central + 5% 1st upwind
SGS model	Standard Smagorinsky Model (Cs=0.1)

Table 2 Boundary conditions

	Velocity	Temperature
Inlet	Inflow turbulence generated by spatial filtering and rescaling method based on WRF-LES results (Figure 5)	
Top, side	Free-slip	Dirichlet
Surface of building, ground	Spalding law	Jurges equation

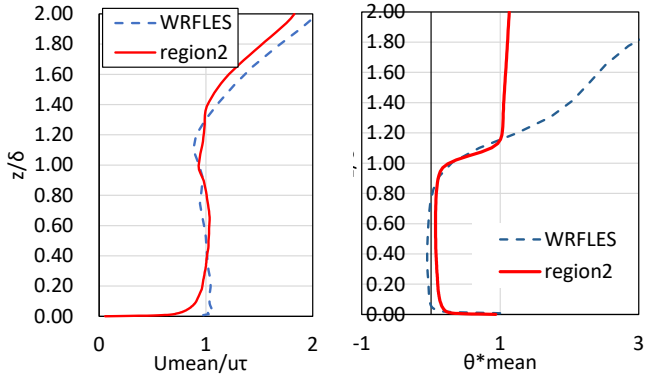

Figure 5: Inflow conditions (vertical distribution of average velocity and average temperature)

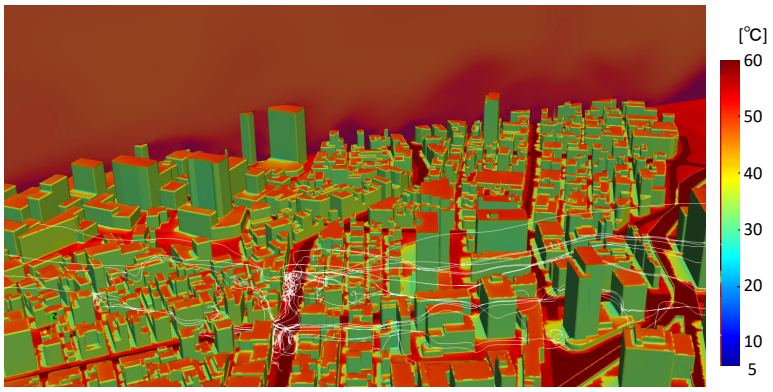

Figure 6: Surface temperatures of building cluster and streamlines of wind flowing into major roads

3.2. Evaluation of thermal environment and heat stress in urban districts

To confirm the thermal environment in urban districts during intense hot day, we examined instantaneous velocity, air temperature, mean radiant temperature (MRT), and WBGT (hereafter referred to as unsteady WBGT) at a height of 1.5 m within the center of urban district area. The unsteady WBGT was calculated from instantaneous values of velocity, air temperature, and MRT. The unsteady WBGT was converted by determining the globe temperature [°C] and wet-bulb temperature [°C] from air temperature [°C], velocity [m/s], and MRT [°C] obtained from numerical simulation results, along with the meteorological observation value for relative humidity (39%). In this study, the existing WBGT formula for outdoor environment (the Ministry of the Environment Government of Japan., 2025 accessed) is used in Eq. (3). The WBGT evaluation classification shows Table 3.

$$WBGT = 0.7T_w + 0.2T_g + 0.1T_a \quad (3)$$

Figure 7 shows the instantaneous distribution of horizontal section at a height of 1.5 m in the central urban area of the analysis region (within the dotted frame in Figure 4(b)). High unsteady WBGT values occur in the area with high air temperature and sunshine, such as along major roads and in low-velocity zones like the wake areas of high-rise buildings. Furthermore, the unsteady WBGT exhibits a similar mesh-like distribution pattern to air temperature. This is likely because the calculation formula for unsteady WBGT has a high contribution rate from wet-bulb temperature, and this report used a model formula for wet-bulb temperature based on air temperature as a function.

Next, Figure 8 shows time-series data for air temperature, velocity, MRT, and unsteady WBGT were compared at three points near the building. The probe locations correspond to the dash-dot line frames in Figure 7. Air temperature, velocity, and unsteady WBGT fluctuated significantly due to the fluctuations of turbulence field, while MRT showed smaller fluctuations and slower temporal changes. Particularly at the corner of the major road intersection (at Point A), where temperature and unsteady WBGT fluctuations were large, the temperature peaked at approximately 40°C, while the unsteady WBGT reached a peak value of approximately 37.5°C compared to a 5-minute time-averaged value of approximately 30.6°C. Based on the above, this analysis method enabled the reproduction of unsteady fluctuations and localized high-temperature occurrences in the thermal environment in the urban area. From the above, it was able to be grasped the detailed spatial-temporal distribution of the heat environment within urban districts to which pedestrians may be exposed.

As an example of evaluating the thermal environment considering environmental fluctuations over a certain elapsed time, we attempted to confirm a value combining the time-averaged value and standard deviation of the unsteady WBGT. To the purpose of evaluating cases where thermal stress on the human body is stronger than average, this paper calculated a value obtained by adding the standard deviation σ to the time-averaged value (hereafter, mean + σ). For reference, Figure 8(a) shows a graph with "mean + σ". When compared to the existing WBGT evaluation ranges. It suggests that the evaluation could potentially increase by one level with large fluctuations periods or locations, such as Point A from 11:45 to 11:50. In future work, by adjusting the statistical processing time of the simulation values to a timescale that considers the accumulation of heat stress on the human body, the development of methods of heat evaluation that account for fluctuations is also expected.

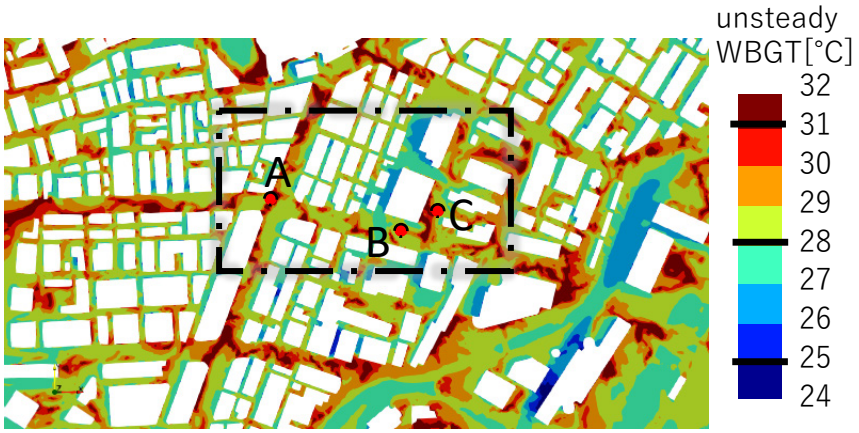

Figure 7 Horizontal distribution of unsteady WBGT within the central urban area (z=1.5m, 11:47)

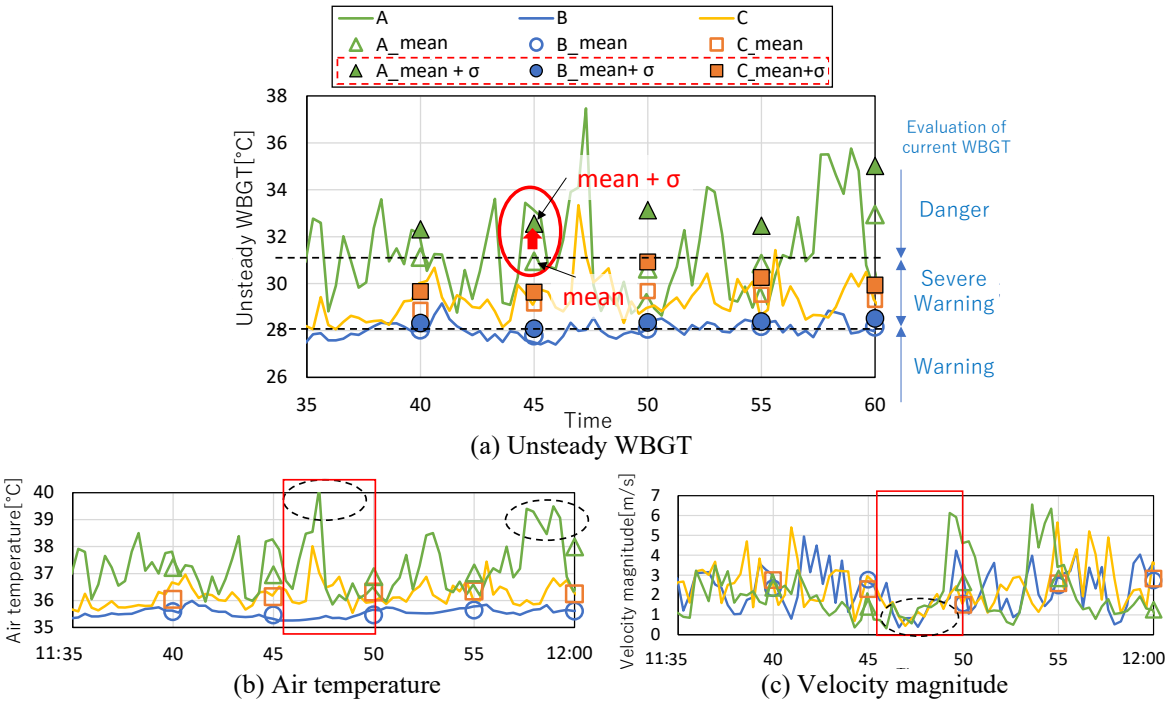

Figure 8: Positions of each point and time-series data for unsteady WBGT, air temperature, velocity (horizontal axis: elapsed time from 11:00)

Table 3: Guidelines for daily life based on the WBGT index
(from the Ministry of the Environment Government of Japan, website, 2025 accessed)

The WBGT index	Guidelines for Daily Activities	Precautions
Danger (31≦WBGT)	Risk present in all daily activities	For the elderly, there is a high risk of heat-related illness even while at rest. Avoid going outside as much as possible and move to a cool indoor location.
Severe Alert (28≦WBGT<31)		Avoid direct sunlight when going outside, and be mindful of rising indoor temperatures.
Alert (25≦WBGT<28)	Risk associated with moderate to heavy daily activities.	Take regular and sufficient breaks when exercising or performing strenuous work.
Caution (WBGT＜25)	Risk associated with strenuous daily activities.	While the risk is generally low, it may occur during intense exercise or heavy labor.

4. CONCLUSIONS

This study conducted coupled analysis of turbulent flow and radiative fields in urban areas using inflow turbulence that account for meteorological disturbances, focusing on the vicinity of the Tokyo District Meteorological Observatory during the 2018 hot event. It evaluated the unsteady thermal environment in densely built-up urban areas and shown significant fluctuations in temperature and unsteady WBGT. Future work will consider incorporating vegetation models (Arai et al., 2024b) into urban district area simulations.

ACKNOWLEDGEMENTS

This research was supported by MEXT as “Program for Promoting Researches on the Supercomputer Fugaku” (Smart Design Realized on the Supercomputer "Fugaku" in the Society 5.0 Era) and used computational resources of the supercomputer Fugaku of HPCI system provided by the RIKEN Center for Computational Science (ID: hp210262).

REFERENCES

Arai, M., Tamura, T., Kawai, H., 2024a. Validation of a Method of Thermal Radiation and LES Coupled Analysis and Applicability to Actual Urban District, J. Environ. Eng., AIJ, Vol.89, No,819, pp.258-26, https://doi.org/10.3130/aije.89.258

Arai, M., Tamura, T., Kawai, H., 2024b. LES Analysis of Turbulent Flow Field Considering Thermal Radiation in Urban Districts, -A Study of Analysis Method Considering the Effect of Trees-, Summaries of Technical Papers of Annual Meeting AIJ, pp.1969-1970

Arai, M., Tamura, T., Kawai, H., 2025. Study of Inflow Turbulence Considering Thermal Instability Based on Meteorological Disturbance in Urban Area, J. Environ. Eng., AIJ, Vol.90, No,827, pp.45-51, https://doi.org/10.3130/aije.90.45

ISO 7933. 2018, Ergonomics of the thermal environment—Analytical determination and interpretation of heat stress using the predicted heat strain model. International Organization for Standardization, Geneva.

Kawai, H., Tamura, T., 2020. Method for Adding High Frequency Components to a Velocity Field Obtained from a Mesoscale Meteorological Model, J. Structural and Construction Eng., AIJ, Vol.85, No.767, pp.19-27, https://doi.org/10.3130/aijs.85.19

Ministry of the Environment Government of Japan., 2025 accessed. Heat Illness Prevention Information, About WBGT (Wet Bulb Globe Temperature), https://www.wbgt.env.go.jp/en/doc_prevention.php

Nozu, T., Tamura, T., 2012: LES of turbulent wind and gas dispersion in a city, Journal of Wind Engineering and Industrial Aerodynamics, 104-106, pp.492–499

Y. Cui, S. Ai, Y. Liu et al., 2020: Hourly associations between ambient temperature and emergency ambulance calls in one central Chinese city: Call for an immediate emergency plan, Science of The Total Environment, 711, 135046, pp.1-8